Surface Deformation in Imperial Valley, CA, From Satellite Radar Interferometry

Mariana Eneva[1], David Adams[1], Giacomo Falorni[2], and Jessica Morgan[2]

[1] Imageair Inc., U.S.A.
[2] TRE Canada Inc., Canada
meneva@imageair-inc.com • dadams@imageair-inc.com
giacomo.falorni@trecanada.com • jesssica.morgan@trecanada.com

Keywords

Satellite radar interferometry, InSAR, PSInSAR, SqueeSAR, subsidence, surface deformation, geothermal, Imperial Valley, Salton Trough, Hudson Ranch, Salton Sea, Heber, East Mesa

ABSTRACT

In a current California Energy Commission (CEC) project, satellite radar interferometry (InSAR) is applied to detect surface deformation in several areas of the Imperial Valley in southern California. These areas include established, new and possible future geothermal fields, as well as nearby fault zones. The InSAR technique used, SqueeSAR^{TM}, is the latest innovation in the field of radar interferometry. It makes it possible to obtain deformation time series at locations of permanent and distributed scatterers (PS and DS), playing the role of numerous benchmarks. The deformation time series are then used to estimate annual deformation rates. The PS represent points aligned along roads and canals, buildings, wellheads, etc., which remain coherent from one satellite image to another. The DS cover several pixels in the satellite scenes and emit weaker signals than the PS, but still above the backscatter noise. The SqueeSAR^{TM} technique works well for vegetated and rural areas and thus provides unique results from the agricultural lands of Imperial Valley. The radar scenes used for the analysis are from the Envisat satellite, over the period 2003-2010. Two data sets were used, consisting of 45 descending and 33 ascending images, for which the satellite moved from north to south and south to north, respectively.

In this paper the focus is on three geothermal fields – Salton Sea (SSGF), Heber (HGF), and East Mesa (EMGF). Preliminary results show that distinct areas of subsidence are seen in all of these fields. Earlier results from a two-year study using data from another satellite for the SSGF, are confirmed in the present work. At the HGF, there is also evidence of uplift.

Radar interferometry provides unprecedented information on surface deformation, with great spatial and temporal detail, which cannot be achieved by any ground-based means. In this capacity, it has applications for pre-production reservoir assessment, ongoing exploration, and mitigation of any environmental impact that might occur.

Introduction

The Imperial Valley extends for about 80 km in southern California, from the southern shore of the Salton Sea toward the U.S. – Mexico border. Together with the Coachella Valley to the north, it is part of the Salton Trough. It is a spreading center associated with the relative movement of the Pacific and North American Plates. Thus it is characterized by active tectonics, with both subsidence and substantial horizontal movements taking place on a regional scale. This is confirmed by current observations at the GPS stations in the region (Figure 1). Local

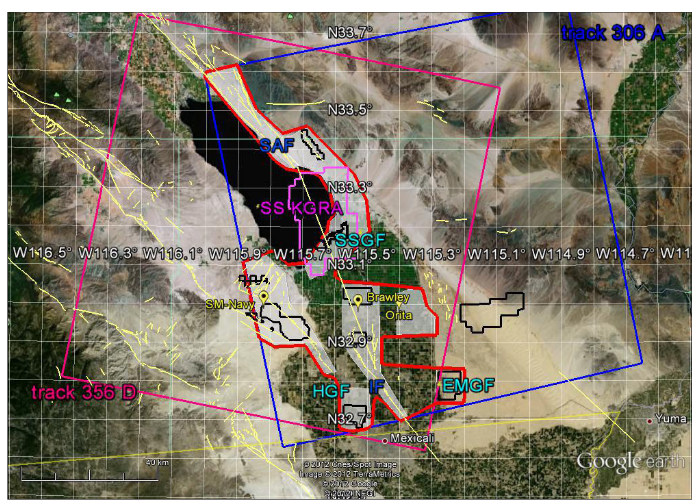

Figure 1a. Study areas in Imperial Valley, CA. Red outline shows the total study area. White polygons show individual study areas. Black outlines show current or known geothermal areas. Light pink outline marks the Salton Sea KGRA. Light blue letters mark geothermal fields studied in this paper – SSGF, HGF, and EMGF (see text). Yellow traces mark faults (USGS, 2006). IF and SAF in dark blue letters denote the Imperial fault and the southern part of the San Andreas fault. Large blue and dark pink rectangles mark the footprints of the ascending (track 3506) and descending (track 356) Envisat scenes. Superimposed on Google Earth.

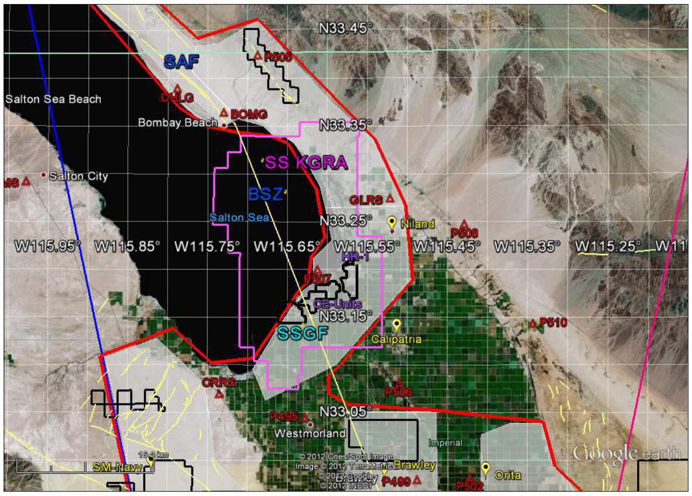

Figure 1b. Northern part of the study area shown in Fig. 1a. Notations are like in Fig. 1a, with the addition of the red triangles marking the GPS stations in the area. The yellow straight line from NW to SE marks the center of the broad Brawley Seismic Zone (BSZ). The CalEnergy units (CE-Units) and the new Hudson Ranch development operated by Energy Source (HR-1), both in the Salton Sea geothermal field (SSGF), are marked with purple letters.

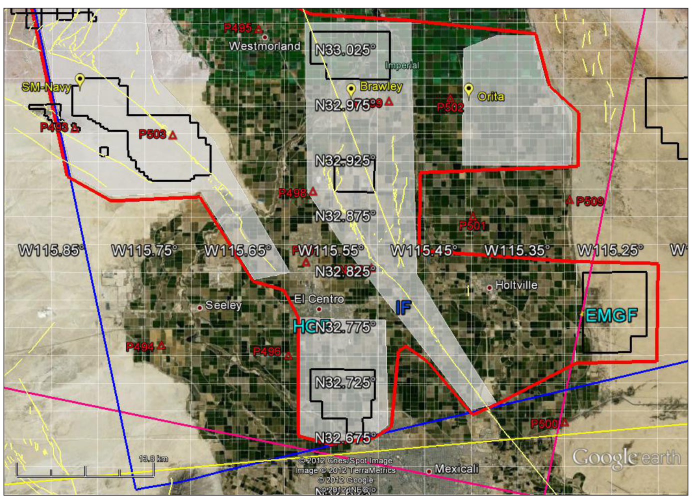

Figure 1c. Southern part of the study area shown in Fig. 1a. Notations are like in Figs. 1a and 1b. SM-Navy marks the area around Superstition Mountain, of interest to the U.S. Navy. This area, along with Orita (East Brawley) and North Brawley, are geothermal areas to be studied in near future under the same CEC project.

sources of deformation are represented by blocks formed by networks of strike-slip and normal faults, many of which do not have surface expression, especially in the agricultural areas. The contribution of local tectonics is likely significant, especially in light of recent studies using seismic reflection data collected from the Salton Sea (Brothers et al., 2009). These authors note that oblique extension across strike-slip faults cause subsidence, leading to the formation of pull-apart basins, such as the Salton Sea and surrounding areas. They project maximum subsidence near the southern shoreline of the sea, approximately coincident with the locations of Quaternary volcanism and a northeast-trending band of very high heat flow.

In addition to the gradual deformation due to regional and local tectonics, the Salton Trough experiences abrupt surface ruptures due to large earthquakes and associated aseismic slip. The Brawley Seismic Zone (BSZ) represents the transitional zone between the southern tip of the San Andreas fault to the northeast, and the Imperial fault to the south (Fig. 1b). It likely includes a number of faults, but they do not have obvious surface expression. Some of these may be related to linear features, as suggested when relocated earthquakes (Hauksson et al., 2012) are displayed in maps and depth cross-sections (see examples below). Brothers et al. (2009) attribute the larger earthquakes ($M > 6$) in the region to the accommodation of the regional extension and subsidence, and the smaller events ($M < 5$) and microseismicity to fracturing and block rotation within narrow (< 5-km-wide), dextral shear zones. Seismic swarms, such as those in 1981, 1989, 2005 and 2009, have been related to the high heat flow in the region (Ben-Zion and Lyakhovsky, 2006). The 2005 M5.1 swarm in particular, which has occurred on the territory of the Salton Sea geothermal field, has been studied in great detail by Lohman and McGuire (2007).

Under a current California Energy Commission (CEC) project, we study several areas in Imperial Valley, of total size 2,328 km^2 (Fig. 1a). The high heat flow here is associated with a number of geothermal resources. The study region includes several current geothermal fields: (1) Salton Sea (SSGF) operated by CalEnergy for more than 30 years, with a new development (Hudson Ranch -1) recently started by Energy Source; and (2) Heber (HGF), North Brawley, and East Mesa (EMGF), operated by Ormat. Other prospective geothermal sites within the study region are the area of Superstition Mountain of interest to the U.S. Navy, and Orita (formerly East Brawley). Areas along faults in proximity to the geothermal sites are also included, such as Imperial, Brawley, and the southern part of the San Andreas faults. The ultimate goal of the CEC project is to describe in detail the surface deformation in all of these areas. In this paper we present preliminary results only for three of the study areas – SSGF, HGF, and EMGF.

Method and Techniques

The method used for mapping surface deformation in Imperial Valley is satellite radar interferometry, also known as interferometric synthetic aperture radar (InSAR). There exist several techniques under this general method. The traditional InSAR technique used for detecting deformation from earthquakes, water pumping, mining, and some geothermal areas, has been differential InSAR (DInSAR) (e.g., see Eneva, 2010 for an overview). In particular, there have been DInSAR observations at some geothermal fields, such as East Mesa in southern California (Massonnet et al., 1997), fields in Nevada (e.g., Oppliger et al., 2008), Coso in eastern California (Wicks et al., 2001; Fialko and Simmons, 2000), and Cerro Prieto in Mexico (Carnec and Fabriol, 1999) south of our study area. However, DInSAR does not work in agricultural areas like Imperial Valley. For such areas, a recent innovation, PSInSAR^{TM} (Ferretti et al., 2000, 2007) is needed. It makes use of so-called "permanent scatterers" (PS) to produce detailed deformation time series and deformation rates. PS are objects, such as buildings, fences, lampposts, transmission towers, rock outcrops, points aligned along roads and canals, etc., which serve as reflectors of the radar waves. We have previously applied the PSInSAR^{TM} technique to detect two distinct subsidence bowls at the Salton Sea geothermal field (Eneva et al., 2009; Eneva and Adams, 2010; Falorni et al., 2011), using 18 ascending and 21 descending images from a Canadian satellite, Radarsat, over the period May 2006 – March 2008.

In the present work we apply the latest improvement of PSInSAR^{TM}, called SqueeSAR^{TM} (Ferretti et al., 2011). In addition to PS locations, this technique makes use of "distributed scatterers" (DS). These are homogeneous areas emitting signals with smaller signal-to-noise ratios than the PS, but still significantly above the background. These include rangelands, pastures, and bare earth characteristic of relatively arid environments. This technique is particularly well suited to study rural areas. Prior to the present work, we have successfully applied SqueeSAR^{TM} to detect deformation at the San Emidio geothermal field in northwestern Nevada (Eneva et al., 2011).

Displacement measurements in any InSAR studies are done relative to a reference point, considered to be stable. This is similar to performing leveling surveys. So, only relatively local movements are measured, rather than regional ones. This has to be kept in mind when viewing the InSAR results, because depending on the reference point, the displacements may be of different amounts, although overall relative patterns of deformation would remain the same. It may not be possible to find truly "motionless" reference points in tectonically active regions like the Salton Trough. Therefore, it would be advantageous to know the absolute movement of the reference points. This can be achieved by using locations of GPS stations as a reference. In our earlier work at the SSGF (Eneva et al., 2009; Eneva and Adams, 2010), a reference point on Obsidian Butte, S-1246, was used, to keep in line with the annual leveling surveys carried out by CalEnergy and to perform direct comparison. However, it was noted that this benchmark actually subsides at close to –20 mm/year. This was established by comparing the vertical displacement recorded at another CalEnergy benchmark, RED-1 (in reference to S-1246), with the "absolute" measurements at a nearby GPS station, P-507. It was clear then that any subsidence slower than that of S-1246 (~ –20 mm/year) would appear as a relative uplift, which was indeed noted in the northeastern part of the SSGF. Here we continue to use S-1246 as a reference when comparing the earlier Radarsat results with the new Envisat results.

The deformation is first measured in the line-of-sight (LOS) to the satellite, either away from it or toward it. When the look angle is steep, the LOS movements are rather representative of the vertical displacements. Thus a LOS movement away from the satellite is mostly subsidence and toward the satellite is mostly uplift. Here imagery from both descending (satellite moves north to south) and ascending (satellite moves south to north) orbits are used. In both cases, the look angle is rather steep. In the previous study using the Radarsat data (Eneva et al., 2009), the look angle was relatively steep only for the ascending orbit, while it was rather oblique for the descending one. This made the descending LOS movements about equally sensitive to the vertical and horizontal movements. So, if we are to compare LOS movements measured by the two satellites, only those from the ascending orbits of Envisat and Radarsat are directly comparable, because of the similarly steep look angles, while the descending movements cannot be compared without decomposition into vertical and horizontal movements.

The availability of scenes from two orbital geometries, ascending and descending, makes it possible to decompose the LOS movements into purely vertical component, and one horizontal component, in the west-east direction. The north-south component cannot be deduced from the LOS movements. The vertical component would be similar to the LOS measurements for steep look angles, as in the case of ascending Radarsat data and both ascending and descending Envisat data. However, only decomposition can reveal the horizontal movements, which are otherwise buried in the LOS measurements. In addition to the two distinct subsidence bowls detected at the SSGF, the presence of significant horizontal movements was shown (Eneva et al., 2009; Eneva and Adams, 2010). As could be expected, the horizontal movements are directed toward the inside of the subsidence areas. This is represented by eastward movements on the western edge and westward movement on the eastern edge of the subsidence (north-south movements cannot be detected by InSAR).

A number of codes were created to examine various aspects of the results. For example, it is possible to study individual polygons of arbitrary size and examine individual and mean time series from the PS and DS in them, to display the deformation rates along profiles of interest, and to superimpose the seismicity on maps and profiles. Some examples are shown below.

Data

Two sets of radar scenes are used in this study, both from the European Envisat satellite. The data were obtained from the European Space Agency (ESA). One data set consists of 45 descending images from track 356, covering the period February 7, 2003 – September 3, 2010. The other one consists of 33 ascending images from track 306, covering the period December 16, 2003 – August 21, 2010. The footprints of the two sets are marked on Fig. 1a. The look angles for the descending images are 21^0 to 22^0, and for the ascending images 20^0 to 21^0 (i.e., they vary slightly over the relatively large study area). The sensitivity of the movements detected in the line-of sight (LOS) is measured with values between 0 and 1, with larger values indicating greater sensitivity. Because of the steep look angles, the LOS movements are rather representative of the vertical surface deformation, with sensitivity ~0.93 for both the descending and ascending images. The sensitivity to the west-east horizontal component of surface deformation is ~0.34-0.37, while the sensitivity to the south-north component is negligible (~0.07-0.08).

Preliminary Results

Because the study area is relatively large, the data were processed separately for its northern and southern portions, using different reference points.

Salton Sea Geothermal Field

Our first focus was to compare the 8-year Envisat results on the territory of the Salton Sea geothermal field (SSGF) with the previous two-year Radarsat results (Eneva et al., 2009; Eneva and Adams, 2010). The look angle for the ascending Radarsat images (~25^0) is quite similar to the Envisat one. For this reason, the LOS movements obtained from the ascending Radarsat and

Envisat scenes can be compared directly. However, the descending Radasat images were with a very different look angle, ~46^0, from that for the descending Envisat scenes, so the descending LOS results cannot be compared without additional calculations (i.e., decomposing into vertical and horizontal movements).

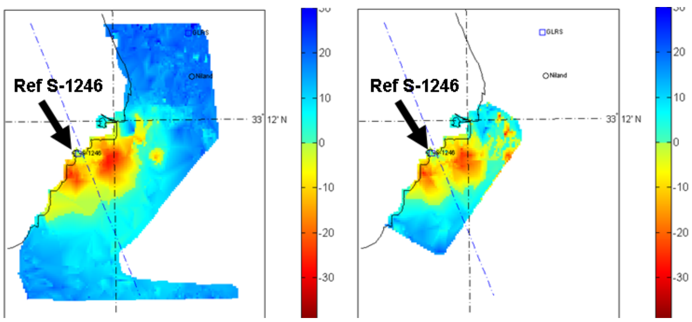

Figure 2. Comparison of the interpolated ascending LOS annual deformation rates between Envisat and Radarsat at the Salton Sea geothermal field for the period May 2006 - March 2008. Left – Envisat rates; right – Radarsat rates (from Eneva and Adams, 2009). Color bars show the rates in mm/year. The reference point is a leveling benchmark on Obsidian Butte used by CalEnergy in their leveling surveys, S-1246. Northwest-southeast dashed line marks the center of the Brawley Seismic Zone (BSZ).

Figure 2 shows the interpolated ascending LOS results for Envisat in this study and Radasat from the previous one (Eneva and Adams, 2010). The Radasat study was much more limited in spatial coverage (~ 60 km^2) compared with the Envisat study here. The Evisat results are shown over a larger area in Fig. 2, specifically extending toward north and north-east, where a new geothermal development, Hudson Ranch-1, operated by Energy Source, is located. To make the comparison more accurate, only two years are shown of the 8 years, for which Envisat imagery is available, choosing the same period, May 2006 – March 2008, as the period covered by the Radarsat data. Subsidence in these maps is shown with "warm" colors, yellow to red. The deformation maps in this figure are referenced to S-1246, to keep in line with the reference benchmark used in the prior study. Fig. 2 shows that the same two subsidence bowls are revealed from applying the SqueeSAR™ technique to the Envisat data, as the ones detected when PSInSAR™ was applied to the Radarsat scenes. What is more, these subsidence bowls persist in time, as they are very similar for two or 8 years of Envisat data (Figure 3). The maximum subsidence rates reach –30 mm/year, in reference to S-1246, so

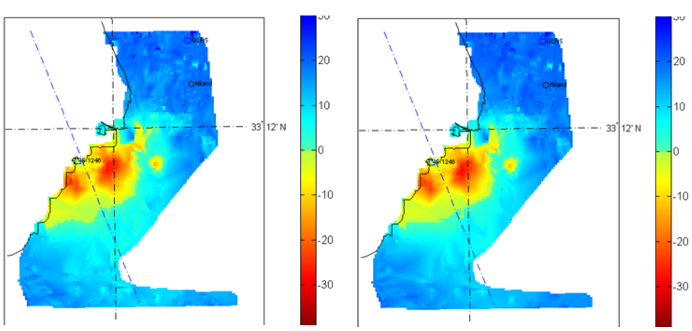

Figure 3. Comparison of two different periods of ascending Envisat LOS annual deformation rates. Left - May 2006-March 2008 (same as left panel in Fig. 2). Right - December 2003-August 2010. Other notations are as in Fig. 2.

if the ~ –20 mm/year subsidence of that benchmark is taken into account the absolute estimate is at ~ –50 mm/year.

As mentioned above, any subsidence slower than the ~20 mm/year, at which S-1246 subsides, would appear as a relative uplift in Figs. 2 and 3 (i.e., in "cold", light to dark blue colors). However, when the reference point is changed to a location with negligible subsidence, the GPS station GLRS with a subsidence at only –1.6 mm/year, the deformation maps show overall subsidence (Figure 4). It is clear that subsidence takes place beyond the limits of the already producing CalEnergy units of the SSGF. That is, subsidence is also seen in the vicinity of the new power plant, Hudson Ranch-1, although at a smaller rate. It decreases from the the new development toward the northeast. This demonstrates the value of our latest results in providing pre-production deformation baselines. Such a baseline does not exist for the already operating plants in SSGF (CalEnergy), and HGF and EMGF (Ormat).

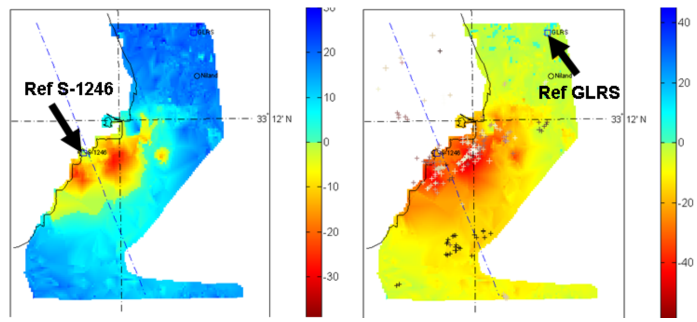

Figure 4. Deformation maps with different reference points. Both plots are for Envisat, May 2006 - March 2008. Left – reference point is S-1246 (like in Figs. 2 and 3). Right - reference point is the location of a GPS station, GLRS. Other notations are as in Fig. 2.

Eneva and Adams (2010) presented an extensive discussion on the possible reasons for subsidence in the CalEnergy area of the SSGF. In summary, we estimated that at most 10% of the maximum deformation can be explained by the regional tectonics. CalEnergy indicates that only a small portion of the total geothermal resource has been exploited, and that minimal pressure changes and no fluid level changes are detected in the wells. This

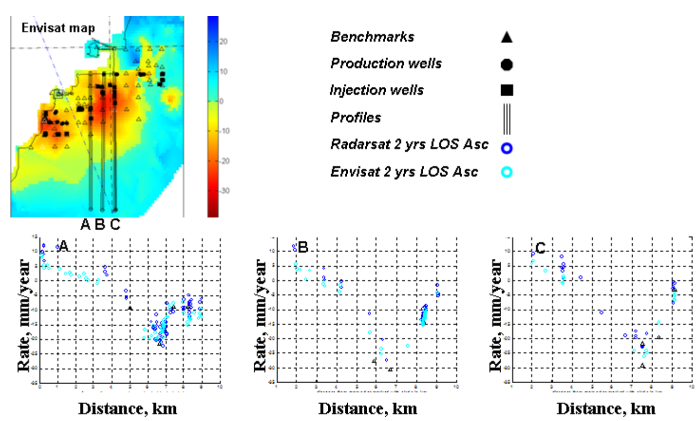

Figure 5. Envisat ascending LOS deformation rates along three profiles across the larger subsidence bowl from Figs. 2 and 3. The legend shows the symbols for the leveling benchmarks used by CalEnergy, production and injection wells, the profiles, and the annual rates from a two-year period for both Radarsat and Envisat. Distance along profiles is from south to north. Other notations are like in Fig. 2.

leads to the suggestion that the reason for the observed surface deformation must be mostly local tectonics.

In addition to the deformation maps shown in Figs. 2-4, it is informative to examine deformation rates along profiles, in small areas including production or injection wells, and superimposed with seismicity. Figure 5 shows and example of deformation rates along thee profiles intersecting the larger subsidence bowl at the SSGF. The profiles from Radasat and Envisat are very similar to each other, as well as compared with benchmark leveling measurements where the profiles pass in the vicinity of such benchmarks. Eneva et al. (2009) have already demonstrated very good agreement between InSAR vertical rates and leveling rates for most of the 79 benchmarks used by CalEnergy.

Figures 6 and 7 show examples of seismicity superimposed on the subsidence bowls in the SSGF. The earthquake catalog used in these plots features relocated events by Hauksson et al. (2012). The magnitude of complete recording for the area appears to be M=2.2 and is used as a magnitude threshold in the left panel of Fig. 6. This value was deduced from magnitude-frequency relationships (not shown). However, epicenters of smaller magnitudes reveal more linear features that may be of interest (right panel of Fig. 6). Focusing along one particular set of linear features in seismicity (Fig. 7), reveals a cross-section in depth indicating shallower hypocenters to the northeast and deeper events to the southwest of the studied polygon. These events might have occurred along the same plane dipping to the northwest, but because of differences in their depths, the southernmost strand of epicenters appears shifted compared with linear features toward the center of the polygon. The majority of earthquakes within this polygon occurred between August and December of 2005, and represents a swarm associated with a September 2005 M5.1 earthquake on the territory of the SSGF.

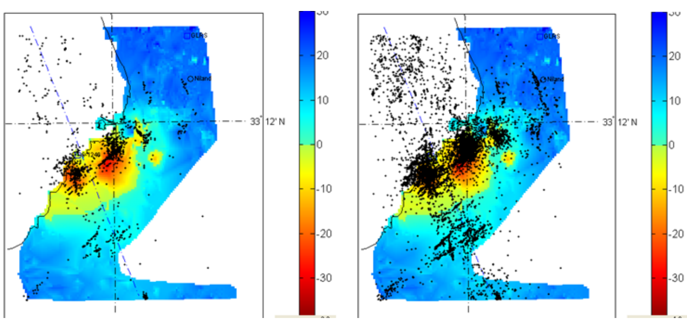

Figure 6. 2003-2010 Envisat ascending LOS deformation maps with 1981-2011 seismicity superimposed. Left: M≥2.2 (magnitude of complete recording). Right: M≥1.0. Notations like in Fig. 2.

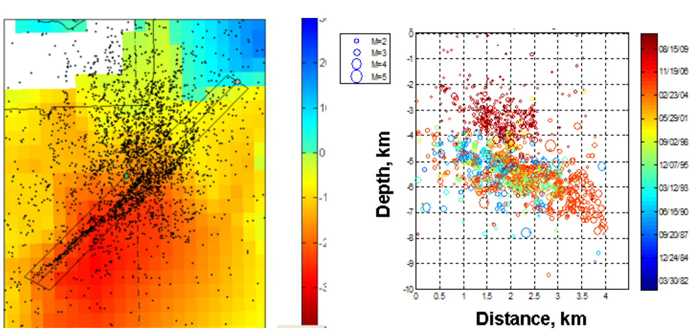

Figure 7. Zoom-in on the LOS deformation map from Fig. 6, with M≥1.0 seismicity. Left – polygon outlining apparent linear trends suggested by seismicity. Right – hypocentral depth cross-section along the polygon, in the NE-SW direction. Most events are from a M5.1 swarm that occurred in the fall of 2005. Color bar for depth cross-section indicates time. Other notations are like in Fig. 2.

Heber Geothermal Field

The Heber geothermal field (HGF), operated by Ormat, is located further to the south, close to the U.S.-Mexico border. To the best of our knowledge, the InSAR results presented here are the first of this kind for this field. Annual leveling surveys are carried out by Ormat at the HGF, using more than 100 benchmarks, but these data are not available yet for comparison with the InSAR results. The number of PS and DS points, at which we have obtained deformation time series, and hence estimates of annual rates, is obviously incomparably larger than the number of benchmarks used in the leveling surveys. Figure 8 shows colored PS points, with the color indicating the amounts of subsidence and uplift. The deformation maps from both the descending and ascending Envisat scenes show uplift in the northern part of the HGF and subsidence to the south. Examples of individual time series at the PS points of maximum uplift and maximum subsidence rates are also shown in Fig. 8. These maximum rates, estimated over the whole 8-year period covered by the Envisat data (2003-2010), are +27 mm/year of uplift and –42 mm/year of subsidence.

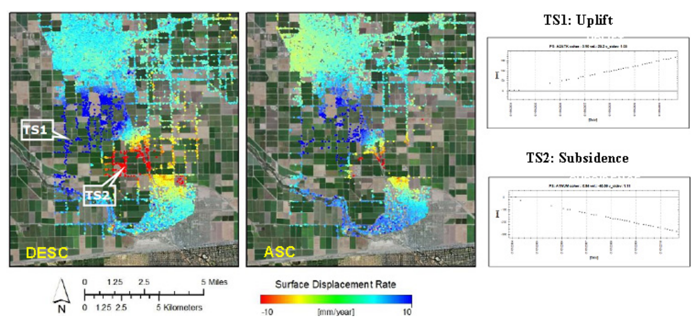

Figure 8. Envisat LOS surface deformation, with examples of uplift and subsidence time series from the Heber geothermal field. The color of the PS points indicates the annual deformation rate according to the color bar on the bottom. Reference points are outside the plots.

East Mesa Geothermal Field

Unlike SSGF and HGF discussed above, our InSAR results are not the first ones for the East Mesa geothermal field (EMGF). This field is outside the agricultural areas, in arid lands, so the conventional DInSAR approach can easily work for it. Indeed, one of the earliest publications documenting the use of DInSAR was about the EMGF (Massonnet et al., 1997). In that work, four pairs of descending scenes were used from the ERS-1 satellite (a predecessor of Envisat), in the period 1992-1994. A maximum subsidence rate of –35 mm/year was estimated.

The earlier DInSAR study used only four descending images over 2 years. So, the SqueeSAR™ technique we applied to 33 Envisat ascending images over 8 years is vastly superior, with its supply of deformation time series at numerous PS and DS locations. Because the area occupied by the EMGF is arid, the density of PS points is very high. Figure 9 shows LOS movements from the ascending Envisat images. Most of the area is subjected to subsidence, with a maximum rate of –29 mm/year.

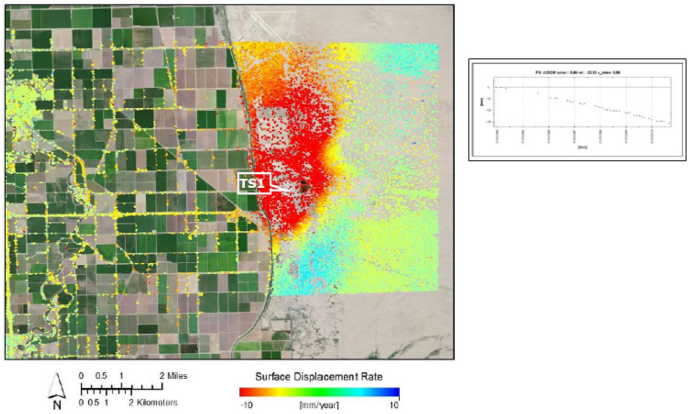

Figure 9. Envisat ascending LOS surface deformation map and an example of a subsidence time series from the East Mesa geothermal field. Notations are like in Fig. 8. Reference point is outside the mapped area shown.

Conclusions

The InSAR technique used here, SqueeSAR^{TM}, has provided unprecedented information on surface deformation in Imperial Valley. Except for the area of the East Mesa geothermal field, no other InSAR techniques could work in this region, because of extensive agriculture. Great spatial and temporal details are revealed, which cannot be achieved by any ground-based means, such as GPS and leveling. This type of results is invaluable with its capability to provide deformation baselines for future geothermal fields in the area. In addition, such results are very informative for the improved understanding of surface deformation in current fields. Thus radar interferometry can find applications in pre-production reservoir assessment, ongoing exploration, and mitigation of any environmental impact that may occur.

Future work under the current California Energy Commission (CEC) project will include more details on the geothermal fields featured here, obtaining results from other prospective geothermal areas, and studying areas along the Imperial fault and the southern portion of the San Andreas fault. We will also proceed to decompose the LOS movements into vertical and horizontal displacements.

Acknowledgements

Support from the Geothermal Grants and Loans Program of the California Energy Commission (CEC), Grant GEO-10-001, is gratefully acknowledged. Many thanks to Alex Schriener and Jon Trujillo from CalEnergy for assuring match share to the CEC grant in the form of digital data from the annual leveling surveys at the Salton Sea geothermal field, helping with the interpretation of the InSAR results, and providing comments on this paper. Danny Sims and Jim Turner from Energy Source are thanked for reviewing the manuscript and providing insight on their new development at the Salton Sea geothermal field, Hudson Ranch-1. The Envisat satellite data were obtained from the European Space Agency (ESA) as part of an approved Category-1 research data proposal. GPS data were taken from the Scripps Orbit Permanent Array Center (SOPAC) – http://sopac.ucsd.edu.

References

Ben-Zion, Y., and V. Lyakhovsky, 2006. “Analysis of aftershocks in a lithospheric model with seismogenic zone governed by damage rheology.” *Geophys. J. Int*., v. 165, p. 197– 210.

Brothers, D.S., N.W. Driscoll, G.M. Kent, A.J. Harding, J.M. Babcock, and R.L. Baskin, 2009. “Tectonic evolution of the Salton Sea inferred from seismic reflection data.” *Nature Geoscience*, v. 2, p. 581-584, doi: 10.1038/NGEO590.

Carnec, C., and H. Fabriol, 1999. “Monitoring and modeling land subsidence at the Cerro Prieto geothermal field, Baja California, Mexico, using SAR interferometry.” *J. Res. Lett.*, v. 26, p. 1211-1214.

Eneva, M., G. Falorni, W. Teplow, J. Morgan, G. Rhodes, and D. Adams, 2011. “Surface deformation at the San Emidio geothermal field, Nevada, from satellite radar interferometry.” *Geothermal Resources Council Transactions*, v 35, p. 1647-1653.

Eneva M., 2010. “Detection of surface deformation at mining and geothermal sites using satellite radar interferometry (InSAR).” In *Proceed. 44th U.S. Rock Mechanics Symposium and 5th U.S.-Canada Rock Mechanics Symposium, Salt Lake City, June 27-30, 2010*.

Eneva M., and D. Adams, 2010. “Modeling of surface deformation from satellite radar interferometry in the Salton Sea geothermal field, California.” *Geothermal Resources Council Transactions*, v. 34, p. 527-534.

Eneva M., G. Falorni, D. Adams, J. Allievi, and F. Novali, 2009. “Application of satellite interferometry to the detection of surface deformation in the Salton Sea geothermal field, California.” *Geothermal Resources Council Transactions*, v. 33, p. 315-319.

Falorni G., J. Morgan, and M. Eneva, 2011. “Advanced InSAR techniques for geothermal exploration and production.” *Geothermal Resources Council Transactions*, v. 35, p. 1661-1666.

Ferretti A., C. Prati, and F. Rocca, 2000. “Nonlinear subsidence rate estimation using permanent scatterers in differential SAR Interferometry.” *IEEE Trans. Geosc. Rem. Sensing*, v. 38, p. 2202-2212.

Ferretti A., G. Savio, R. Barzaghi, A. Borghi, S. Musazzi, F. Novali, C. Prati, and F. Rocca, 2007. “Submillimeter accuracy of InSAR time series: Experimental validation.” *IEEE Trans. Geosci. Rem. Sensing*, v. 45, p. 1142-1153.

Ferretti A., A. Fumagalli, F. Novali, C. Prati, F. Rocca, and A. Rucci, 2011. “A new algorithm for processing interferometric data-stacks: SqueeSAR.” *IEEE Trans. Geosc. Rem. Sensing*, v. 49, No 9, p. 3460-3470.

Fialko, Y., and M. Simmons, 2000. “Deformation and seismicity in the Coso geothermal area, Inyo County, California: Observations and modeling using satellite radar interferometry.” *J. Geophys. Res.*, v. 105, p. 21,781-21,793.

Hauksson, E., W. Yang, and P.M. Shearer, 2012. “Waveform relocated earthquake catalog for southern California (1981 to 2011)”, submitted to *Bull. Seismol. Soc. Am.*

Lohman, R. B., and J. J. McGuire, 2007. “Earthquake swarms driven by aseismic creep in the Salton Trough, California. “ *J. Geophys. Res.*, v. 112, B04405, doi:10.1029/2006JB 004596.

Massonnet, D., T. Holzer, and H. Vadon, 1997. “Land subsidence caused by the East Mesa Geothermal Field, California, observed using SAR interferometry.” *Geophys. Res. Lett.*, v. 24(8), p. 901–904, doi:10.1029/97GL00817.

Oppliger, G., L. Shevenell, and M. Coolbaugh, 2008. “Preliminary site assessment of the Redfield Campus, Reno, NV, USA.” *Geothermal Research Council Trans*, v. 32, p. 163-168.

U.S. Geological Survey (California Geological Survey), 2006. “Quaternary fault and fold database for the United States, accessed October 2011, from USGS web site: http//earthquakes.usgs.gov/regional/qfaults.